

**EFFECTIVE LIFETIME VARIATIONS SIGNIFICANT FOR PROCESS EVALUATION OR JUST AN  
ARTIFACT OF WAFER SIZE AND QUALITY?  
– AN ATTEMPT TO QUANTIFY MATERIAL INDUCED VARIATIONS**

Christian Fischer, Andreas Schmid, Annika Zuschlag, Giso Hahn  
University of Konstanz, Department of Physics, 78457 Konstanz, Germany  
christian.fischer@uni-konstanz.de, Tel: +49 7531 884995, Fax: +49 7531 883895

**ABSTRACT:** Small sample size and usage of sister wafers in photovoltaics research are quite common. Regarding sample size, edge effects and reduced thermal mass may influence applicability of scientific findings to industrial wafers. Therefore, an extended investigation of these effects performed on various Si materials for solar cells can help to evaluate possible drawbacks of small-sized research samples. In addition to problems with inversion-based passivation mechanisms, edge recombination effects can significantly reduce lifetimes. These effects are more detrimental for small-sized samples due to a higher edge-to-area ratio.

Furthermore, a comparison of sister wafers including their degradation and regeneration behavior should help to quantify the uncertainty due to wafer quality variations. Comparable lifetimes without significant variations are shown with annealed sister wafers. However, fired p-type Cz-Si sister wafers are prone to BO and LeTID degradation. Therefore, differing initial lifetimes can be explained by different states of degradation at the start of investigation. Normalized defect densities show comparable maxima referring to regenerated lifetimes.

**Keywords:** Defect Density, Degradation, Lifetime

## 1 INTRODUCTION

Research in photovoltaics is often performed on samples smaller than typical full-size wafer formats. In general, most scientific findings are independent of sample size. However, Veith-Wolf et al. reported for n-type Si wafers passivated by  $\text{AlO}_x$  a dependence of the effective excess minority charge carrier lifetime  $\tau_{\text{eff}}$  on the wafer size [1]. In addition to edge effects, there are further variations induced by sample size. This can be due to chemical etching or high temperature steps like firing. For the firing step, e.g., reduced thermal mass of small samples has to be considered for transferability of results achieved on small samples. Therefore, experiments with  $50 \times 50 \text{ mm}^2$  samples and full-size wafers are performed to determine process steps with size dependency and to quantify the variance.

## 2 EXPERIMENTAL

$156 \times 156 \text{ mm}^2$  Phosphorus-doped ( $\sim 2.3 \Omega \text{cm}$ ) and Boron-doped ( $\sim 2.1 \Omega \text{cm}$ ) Cz-Si wafers with defined ingot position and wafer orientation were used. According to Fig. 1 three groups of wafers were processed. Group I was processed as full-size wafer, group II was laser cut to  $50 \times 50 \text{ mm}^2$  samples before any other process step and group III was cut to  $50 \times 50 \text{ mm}^2$  samples after wet chemical processing. Standard chemical processing was KOH and CP ( $\text{HNO}_3$ ,  $\text{CH}_3\text{COOH}$ , HF) etch to remove saw-damage and polish the sample surface followed by Piranha cleaning and HF-dip. For group III, an additional chemical cleaning step including CP etching of about  $2 \mu\text{m}$  per side was added after cutting to remove potential surface damage due to size adjustment.

All wafers were passivated with an atomic layer deposited (ALD) aluminum oxide ( $\text{AlO}_x$ ). Two types of  $\text{AlO}_x$  were used. One is optimized for annealing (deposition at  $170^\circ\text{C}$ ) and the other for firing (deposition at  $300^\circ\text{C}$ ). For annealing, samples were kept under low pressure in  $\text{N}_2$  atmosphere at about  $420^\circ\text{C}$  for 30 minutes. For firing, a belt furnace was used and set to  $800^\circ\text{C}$  peak

temperature. The actual sample temperature was recorded via a thermocouple pressed on the wafer.

After passivation, samples were characterized via photo conductance decay (PCD) measurement at room temperature and photo-luminescence (PL) imaging. Some samples were treated at elevated temperature ( $130^\circ\text{C}$ ) and 1 sun illumination to check for degradation and regeneration behavior. For the repeated measurement of  $\tau_{\text{eff}}$  at elevated temperature ( $130^\circ\text{C}$ ) a *Sinton Lifetime Tester WCT-120TS* was used.

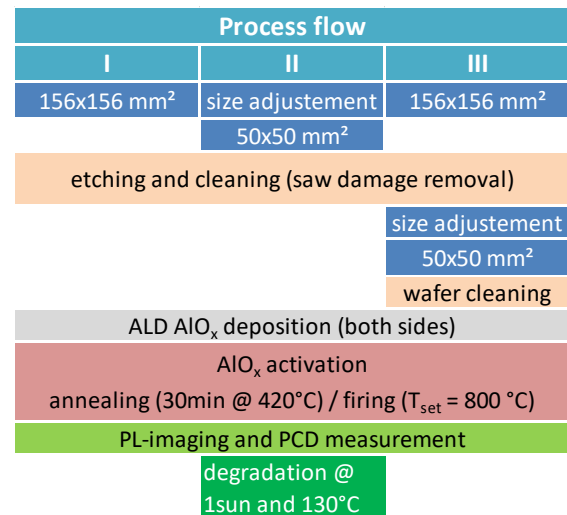
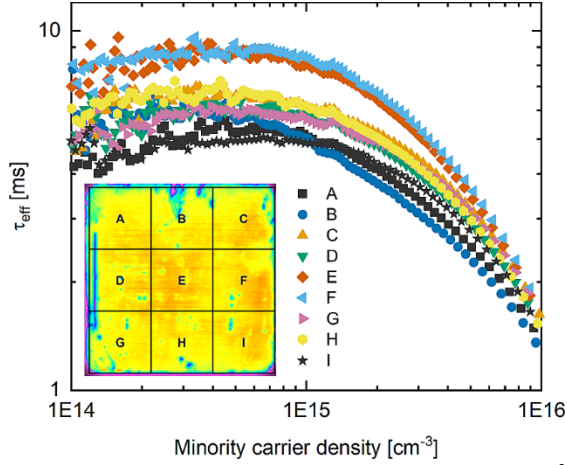


**Figure 1:** Process sequence of the investigated lifetime samples.

## 3 RESULTS AND DISCUSSION

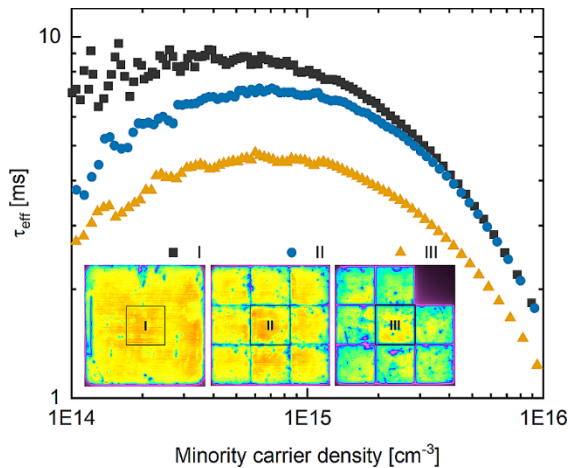
Fig. 2 shows the distribution of effective minority charge carrier lifetimes  $\tau_{\text{eff}}$  from PCD measurements on a  $156 \times 156 \text{ mm}^2$  P-doped wafer and the homogeneity of the passivation. The PL image shows a tweezer mark in the top area (position B). Position E in the center of the wafer is

not influenced by any edge effects and therefore shows the highest  $\tau_{\text{eff}}$ . This is in accordance with literature [1,2]. Therefore, we use this center position for further investigations.



**Figure 2:**  $\tau_{\text{eff}}$  measured by PCD on one 156x156 mm<sup>2</sup> sample from group I (n-type 2.3  $\Omega\text{cm}$  Cz – annealed  $\text{AlO}_x$  passivation) with PL image as inset, where PCD measurement positions are marked.

In Fig. 3 P-doped samples from groups I, II, and III are compared. I is identical to position E in Fig. 2 and therefore not influenced by edge effects. Samples from groups II and III show an injection dependent lifetime behavior, as reported in [1] and [2] for small sized samples.  $\tau_{\text{eff}}$  values from group II exceed significantly the ones of the sample from group III. A possible explanation are contaminations introduced by the laser cutting that could not be removed from sample III by the additional 2  $\mu\text{m}$  etch and wafer cleaning. Further experiments with more surface removal could help to identify this.



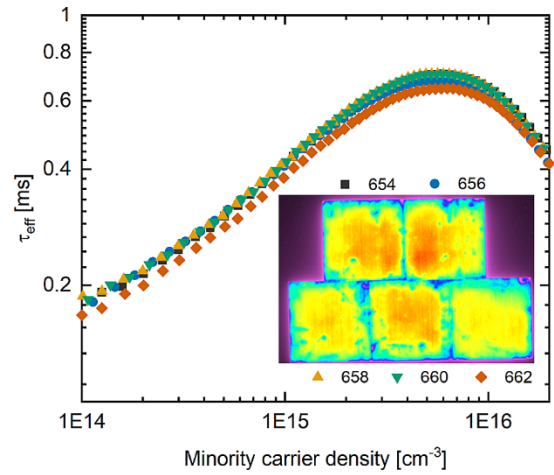
**Figure 3:**  $\tau_{\text{eff}}$  measured by PCD with PL images of three samples (n-type 2.3  $\Omega\text{cm}$  Cz – annealed  $\text{AlO}_x$  passivation) from groups I, II and III with marked measurement spot.

Fig. 4 shows five Boron-doped samples from one ingot processed according to group II. The numbers (654-662) are corresponding to the wafer position in the ingot. So, there is one adjacent sister wafer between two investigated samples with the same process. All wafers

are from the center of a 156x156 mm<sup>2</sup> wafer (position E). The deviation in  $\tau_{\text{eff}}$  determined by PCD between those wafers is within the uncertainty of the measurement. Therefore, a similar behavior for the directly adjacent wafers (653-661) can be concluded. Those adjacent wafers were fired and treated at elevated temperature and illumination. The actual peak sample temperature during firing was recorded and is given with the interstitial iron concentration  $[\text{Fe}_i]$  in Table I.

**Table I:** Measured wafer peak temperatures during firing and determined concentration of interstitial iron (p-type 2.1  $\Omega\text{cm}$  Cz).

| Number | Firing temperature [ $^{\circ}\text{C}$ ] | $[\text{Fe}_i]$ [ $\text{cm}^{-3}$ ] |
|--------|---|--------------------------------------|
| 653    | 775                                       | $3.5 \cdot 10^{10}$                  |
| 655    | 770                                       | $5.2 \cdot 10^{10}$                  |
| 657    | 776                                       | $4.7 \cdot 10^{10}$                  |
| 659    | 773                                       | $2.7 \cdot 10^{10}$                  |



**Figure 4:**  $\tau_{\text{eff}}$  measured by PCD with PL images of five samples (p-type 2.1  $\Omega\text{cm}$  Cz – annealed  $\text{AlO}_x$  passivation – group II) in vertical succession.

Fig. 5 shows the lifetime-equivalent defect density ( $\Delta N_{\text{leq}}$ ) determined from degradation and regeneration cycles during illumination (1 sun, 130 $^{\circ}\text{C}$ ).

$$\Delta N_{\text{leq}} = \frac{1}{\tau_{\text{eff},A}(t)} - \frac{1}{\tau_{\text{eff},B}(t_x)}$$

Normally,  $\tau_{\text{eff}}$  of the first measurement point ( $t_x=0$  h) is chosen for  $\tau_{\text{eff},B}$ . According to Fig. 5, samples 653, 655, 657 show a similar degradation and regeneration behavior. Sample 659 shows a reduced  $\Delta N_{\text{leq}}$  level. This seems to be uncommon for sister wafers.

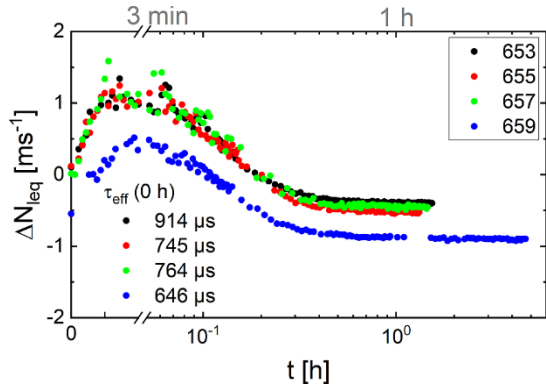


**Figure 5:** Lifetime-equivalent defect density  $\Delta N_{leq}$  of four fired samples (p-type 2.1  $\Omega\text{cm}$  Cz) during treatment at 130°C and 1 sun illumination for about 1 h determined at  $\Delta n=10^{15} \text{ cm}^{-3}$ . Initial effective lifetime values, which were used to determine  $\Delta N_{leq}$  in this graph, are also given.

Therefore, in Fig. 6  $\Delta N_{leq}$  was calculated with the effective lifetime after 1 h of treatment as reference ( $\tau_{eff,B}(t_x=1 \text{ h})$ ). The new calculation results in similar maximum  $\Delta N_{leq}$  values for all samples.

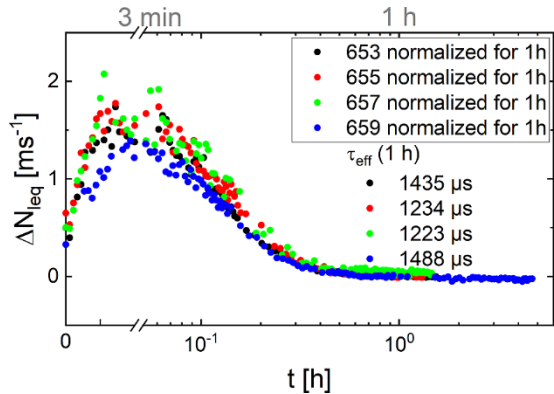


**Figure 6:** Lifetime-equivalent defect density  $\Delta N_{leq}$  of four fired samples (p-type 2.1  $\Omega\text{cm}$  Cz) during treatment at 130°C and 1 sun illumination for about 1 h determined at  $\Delta n=10^{15} \text{ cm}^{-3}$  (same samples as shown in Fig. 5). Effective lifetime values after 1 h, which were used to determine  $\Delta N_{leq}$  in this graph, are also given.

A possible explanation for the observed behavior is that sample 659 was at the beginning of the measurement probably already in an undefined state of degradation. This explains the lower  $\tau_{eff}$  compared to the other sister samples. The regenerated state is for all sister wafers similar as expected (very similar  $\tau_{eff}$  values). Therefore, calculation of  $\Delta N_{leq}$  from the value of  $\tau_{eff}$  after 1 h of treatment time seems reasonable, as defect densities are already stable for all investigated samples.

The observed degradation and regeneration might be an overlap of BO (boron-oxygen) degradation [3] and the LeTID (light and elevated temperature induced degradation) effect, as fired  $\text{AlO}_x$  passivated samples are known to show LeTID [4].

#### 4 SUMMARY

Regarding lifetime measurements on full-size wafer format, measurement spots closer to wafer edges showed

reduced values of  $\tau_{eff}$  due to edge recombination effects. Smaller samples of 50x50 mm<sup>2</sup> showed even lower effective lifetimes, as a) their edge-to-area ratio is larger and b) for an inversion-based passivation mechanism the distance of the measurement spot to the edge(s) plays an important role [1, 2]. But the extent of this effect is significantly influenced by process sequence as well. When size adjustment was performed as the first process step, small samples showed only a small edge effect and slightly reduced  $\tau_{eff}$  compared to a full-size wafer. But size adjustment after etching and cleaning had a detrimental effect on effective lifetime, even when 2  $\mu\text{m}$  are etched off after laser cutting.

Comparing sister wafers, lifetime variations were non-significant as they were smaller than uncertainty of the PCD measurement. However, a group of adjacent wafers showed differences in lifetime-equivalent defect density ( $\Delta N_{leq}$ ) during degradation and regeneration. A calculation of  $\Delta N_{leq}$  normalized by the regenerated value of effective lifetime after 1 h of temperature treatment was performed. With this calculation it was possible to show that in general the  $\Delta N_{leq}$  levels in sister wafers are very similar as expected. Samples did not start at the same level of degradation due to sensitivity to BO and LeTID influencing parameters like temperature and illumination before start of the measurement. Therefore, it is reasonable to normalize on a known common state for all samples like maximum degradation or after regeneration, when calculating  $\Delta N_{leq}$ .

#### 5 ACKNOWLEDGEMENTS

Part of this work was supported by the German BMWi under contract 0324204B. The content of the publication is the responsibility of the authors. The authors would like to thank L. Mahlstaedt, J. Engelhardt and B. Rettenmaier for technical support.

#### 6 REFERENCES

- [1] B. Veith-Wolf et al., Sol. Energ. Mat. Sol. Cells 120, 436-440, 2013.
- [2] C.E. Chan et al., IEEE J. Photovolt. 4, 100-106, 2014.
- [3] A. Herguth and G. Hahn, J. Appl. Phys. 108, 114509, 2010.
- [4] F. Kersten et al., Energy Proc. 92, 828-832, 2016.